Exchange-Collision Technique for the rf Spectroscopy of Stored Ions*†

F. G. MAJOR‡ AND H. G. DEHMELT
Department of Physics, University of Washington, Seattle, Washington 98105
(Received 6 September 1967)

A description is given of a technique, whose application to He^+ has previously been briefly reported, whereby the rf spectrum of field-confined paramagnetic ions in ultrahigh vacuum is observed through spin-dependent collision processes with a spin-polarized beam of neutral particles. A rf electric quadrupole ion trap is used, and a description of the ion motion, based on the adiabatic approximation, is given, including the effect of randomizing elastic collisions with neutral background particles. With particular reference to the $(He^3)^+$-Cs system, the rate equations for the magnetic sublevel populations for an ion with $I=\frac{1}{2}$, $J=\frac{1}{2}$ are derived under the simultaneous action of spin exchange and spin-dependent charge exchange with an alkali atom. According to these equations, the relative intensities observed in the $\Delta F=0$ transitions of $(He^3)^+$ indicate that a Cs spin polarization of 0.5 was achieved in the optically pumped atomic beam. The He^+ polarization approached that of the Cs atoms. With on-off modulation of the Cs polarization, a total 2% change in the He^+ lifetime was observed, with a signal-to-noise ratio of 4, in an interaction period having a duration of 0.8 sec, the optimum value for the observed 0.4-sec lifetime against Cs-induced ion loss. In the absence of the beam, the lifetime was 8 sec at a residual pressure of 3×10^{-8} Torr. The $\Delta F=0$ lines obtained with long integration times had a signal-to-noise ratio which indicated that the $\Delta F=\pm1$ transitions should be observable, as has since been demonstrated.

I. INTRODUCTION

THE preparation of an ensemble of free ions with an over-all electron spin polarization, and the detection of rf transitions by the attendant change in this polarization, requires novel techniques—for the containment of the particles and for the production and analysis of the polarization. This article attempts to provide a fuller account of such techniques, first demonstrated for the He^+ ion, than has previously been published[1,2] on the subject.

The motivation for this work on the He^+ ion springs from two sources: (1) intrinsic interest in the ion as a hydrogenic system for which precise comparison of the predictions of current theory and experimental observations can be made, and (2) general interest in the high spectral resolution which may be realized using a system of electrodynamically suspended ions. A circumstance which sharpens the former interest is that from the work of Novick and Commins[3] the value of the hfs splitting is available for the metastable $2^2S_{1/2}$ state of $(He^3)^+$. The ratio of this value to that for the ground state can be compared with a theoretical value which can be derived with finer precision than either hfs splitting separately because of nuclear-structure effects.[4] The latter source of interest arises since, with the degree of ultrahigh vacuum already attainable in the laboratory, the suspension times of ions in electromagnetic fields are orders of magnitude longer than hitherto possible in the containment of neutral atomic systems. Moreover, the effect of the trapping electromagnetic field on the magnetic spectrum of an ion is very small[5] and more accurately predictable than the case of atoms colliding with the complex surface structure of a storage bulb.

The present techniques are an outgrowth of the work by one of the authors on the g factor of free electrons, in which he introduced orientation by electron exchange into rf spectroscopy, and of his anticipation of the usefulness of ion storage in this branch of physics.[6] The He^+-ion experiment represents the first successful application of electromagnetic-field confinement of ions in ultrahigh vacuum for exploitation of spin-dependent collision processes in their rf spectroscopy. It marks a notable advance in the degree of isolation of the atomic systems under study over that achieved in the earlier experiment on the electrons, insofar as these were contained by the positive-ion cloud of a lightly ionized high-density buffer gas. In essence, He^+ ions, formed by electron impact from residual He gas in an ultrahigh vacuum system, are confined by a high-frequency quadrupole electric field and allowed to undergo spin-exchange collisions with oriented atoms. Thereby the ions become oriented. The atomic species (Cs) is chosen for the high expected spin dependence of simultaneous charge-exchange processes. The atoms are given a high degree of spin polarization by optical pumping[7] before entering the region of confinement of the ions. Conse-

* Based in part on work originally submitted by F. G. M. as a thesis in partial fulfillment of the requirements for the doctoral degree at the University of Washington.

† Supported by grants and contracts from the U. S. Army Research Office (Durham), the National Science Foundation, and the U. S. Office of Naval Research.

‡ Present address: NASA Goddard Space Flight Center, Greenbelt, Md. 20771.

[1] H. G. Dehmelt and F. G. Major, Phys. Rev. Letters **8**, 213 (1962).

[2] E. N. Fortson, F. G. Major, and H. G. Dehmelt, Phys. Rev. Letters **16**, 221 (1966).

[3] R. Novick and E. D. Commins, Phys. Rev. **111**, 822 (1958).

[4] Morton M. Sternheim, Phys. Rev. **130**, 211 (1963).

[5] R. D. Haun, Jr., and J. R. Zacharias, Phys. Rev. **107**, 107 (1957).

[6] H. G. Dehmelt, Phys. Rev. **103**, 1125 (1956); **109**, 381 (1958); Optical Pumping Symposium, 123rd AAAS Meeting, New York, 1956 (unpublished).

[7] A. Kastler, J. Phys. Radium **11**, 255 (1950).

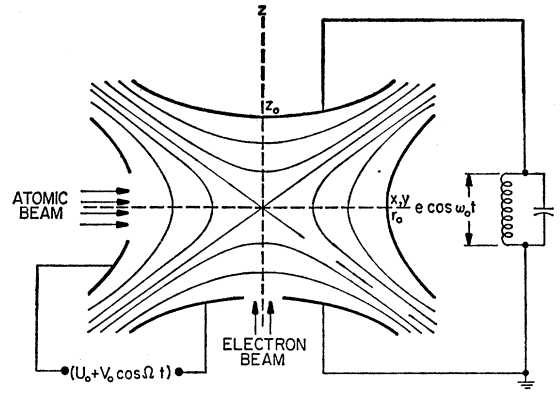

FIG. 1. The rf quadrupole-ion trap showing schematically electrical potential distribution associated with the trapping voltage $U_0+V_0\cos\Omega t$ and where particles enter. The voltage $e\cos\omega_0 t$ is induced in the resonant circuit by the cooperative motion of the ions and allows their detection.

quently the time evolution of the populations of the various magnetic substates of the ions, and in particular the total population, will depend on the presence or absence of induced rf transitions between those substates. Hence, by monitoring the ion lifetime, the magnetic resonance spectrum of the ions can be observed. Our technique may also be viewed as related to Bloch and Alvarez's experiment[8] on the magnetic moment of the neutron. This was the first instance in which collisional orientation—by means of the magnetic interaction between neutron and ferromagnetic polarized atoms—was used in rf spectroscopy. Other members of this group of collisional orientation schemes are electron impact,[6,9] optical pumping,[7] and selective photodissociation. The latter has recently served in other experiments, based on the ion-storage–collision technique like the present one, to observe part of the $\Delta F=0$, ±1 magnetic resonance spectrum of the H_2^+ ion.[10,22]

II. ION CONFINEMENT IN rf QUADRUPOLE FIELD

Among the various devices which use electromagnetic fields for ion suspension, the purely electric rf quadrupole cage of Paul *et al.*[11] was chosen since it leaves open the choice of magnetic fields to fit the needs of rf spectroscopy. In particular, it allows the use of an arbitrarily weak field, in contrast with the static-quadrupole-electric–uniform-axial-magnetic-field combination, the Penning gauge configuration.

The field is described by the following solution of the Laplace equation in cylindrical coordinates (retardation effects are negligible):

$$\phi=r_0^{-2}(U_0+V_0\cos\Omega t)(\tfrac{1}{2}r^2-z^2),\quad \tfrac{1}{2}r_0^2=z_0^2. \tag{2.1}$$

In order to establish such a field in a finite region suitable for the three-dimensional confinement of ions, conducting sheets are placed along a set of equipotential surfaces surrounding the origin as shown in Fig. 1. Clearly, the electrically symmetric choice $r_0^2/2=z_0^2$ made above is not basically necessary, and it may in certain practical applications be more convenient to take an asymmetric electrode arrangement. Moreover, the desired field configuration may be approximated near the origin even with electrodes which have only the symmetry properties of the quadrupole field.

The motion of a charged particle of a given charge-to-mass ratio e/m acted on by such a field is governed by equations of the Mathieu type having the canonical form

$$d^2x_i/d\tau^2+(a_i+2q_i\cos2\tau)x_i=0,\quad x_1=r,\quad x_3=z \tag{2.2}$$

where $\tau=\frac{1}{2}\Omega t$, $a_r=4eU_0/(mr_0^2\Omega^2)$, $a_z=-2a_r$, $q_r=2eV_0/(mr_0^2\Omega^2)$, and $q_z=2q_r$. On the basis of the established theory of the Mathieu equation, its solution is stable or unstable depending on the coefficients a and q. Hence the motion of the ion will be bounded for a given coordinate if the values of U_0, V_0, and Ω are chosen so that the corresponding values of a and q lie within the stable regions of the a-q plane. To facilitate the determination of these physical parameters for simultaneous stable motion in both their r and z directions, Paul *et al.* use the relationships $a_z=-2a_r$, $q_z=2q_r$ to construct, say, in the a_z-q_z plane, a composite plot of the regions of stability for both the z motion and, by proper scaling, for the r motion. Such a stability diagram for the first stable region, where it is most practicable to operate, is reproduced in Fig. 2. In such a region the solution to the equations of motion has the form

$$x(\tau)=A\sum_{-\infty}^{+\infty}c_n\cos(2n+\beta)\tau+B\sum_{-\infty}^{+\infty}c_n\sin(2n+\beta)\tau, \tag{2.3}$$

where c_n and β are functions only of the parameters a and q, and the coefficients A and B are of course determined by the initial conditions. The spectrum of the motion for a given coordinate consists of the following discrete set of frequencies:

$$\omega_n=(n\pm\tfrac{1}{2}\beta)\Omega, \tag{2.4}$$

of which ω_0 will be dominant if a, $q\ll1$, for then the c_n converge rapidly to zero with increasing n. It will be shown later (see the discussion of the adiabatic approximation at the end of this section) that under the condition $q\ll1$, β, and hence ω_0, may be computed from the approximate relationship

$$\beta^2=(a+\tfrac{1}{2}q^2). \tag{2.5}$$

[8] L. W. Alvarez and F. Bloch, Phys. Rev. **57**, 111 (1940).
[9] W. E. Lamb, Jr., and R. C. Retherford, Phys. Rev. **72**, 241 (1947).
[10] K. B. Jefferts and H. G. Dehmelt, Bull. Am. Phys. Soc. **7**, 432 (1962). See also C. B. Richardson, K. B. Jefferts, and H. G. Dehmelt, Phys. Rev. **165**, 80 (1968).
[11] W. Paul, O. Osberghaus, and E. Fischer, Forschungsber. Wirtsch. Verkehrsministeriums Nordrhein-Westfalen No. 415 (1958); E. Fischer, Z. Physik **156**, 1 (1959).

To provide a simple picture of the motion, let it be assumed that $a=0$, and $q\ll 1$, which implies $\beta\ll 1$. Then, neglecting all terms in Eq. (2.3) beyond $n=1$, and taking the initial conditions to correspond to $B=0$, we have

$$x(\tau)=A[c_{-1}\cos(2-\beta)\tau+c_0\cos\beta\tau+c_{+1}\cos(2+\beta)\tau]. \quad (2.6)$$

Now it may be shown that for the assumed values of a and q, it holds

$$c_{-1}\simeq c_{+1}\simeq q/4, \quad \text{for} \quad c_0=1. \quad (2.7)$$

Thus, after regrouping the terms in Eq. (2.6), we have

$$x(\tau)=A(1+\tfrac{1}{2}q\cos 2\tau)\cos\beta\tau. \quad (2.8)$$

Recalling that $\tau=\frac{1}{2}\Omega t$, this clearly represents a harmonic oscillation at frequency ω_0 on which is superposed a ripple at frequency Ω whose amplitude is a constant fraction of the displacement. An important result may be obtained in this approximation concerning the kinetic energy. Thus, on taking the time derivative of Eq. (2.8), squaring, and averaging over a period of the high-frequency field, one finds

$$\langle\dot{x}^2\rangle_{\text{av}}=A^2\beta^2\sin^2\omega_0 t+\tfrac{1}{2}A^2q^2\cos^2\omega_0 t. \quad (2.9)$$

Since for $a=0$, $\beta^2=\frac{1}{2}q^2$, it is evident that in this case the kinetic energy averaged over the Ω oscillation remains constant as the ion executes its low-frequency ω_0 oscillation in the trap: It merely alternates between the high-frequency motion and the low-frequency motion as the ion goes from regions of large rf field amplitude to regions of small amplitude.

Since the application of field confinement to the rf spectroscopy of ions generally implies the presence of a uniform magnetic field, it is necessary to examine the effect of such a field on the motion of the ions. In the case of a uniform axial magnetic field H_0, it is well known that the transformation

$$\rho_+=x+iy, \quad \rho_-=x-iy, \quad z'=z \quad (2.10)$$

uncouples the equations of motion. Here the solution of the uncoupled equations is of the form

$$\rho_\pm=r\exp(\pm i\omega_L t), \quad \omega_L=eH_0/2mc \quad (2.11)$$

where r is a solution of

$$d^2r/dt^2+(\omega_L^2+\tfrac{1}{4}a_r\Omega^2+\tfrac{1}{2}q_r\Omega^2\cos\Omega t)r=0. \quad (2.12)$$

On writing

$$a_r'=a_r+4\omega_L^2/\Omega^2, \quad (2.13)$$

it is seen that the effect of a uniform axial magnetic field is simply to alter the value of the coefficient a_r by an amount $4\omega_L^2/\Omega^2$ and to give the following spectrum [see Eq. (2.4)]:

$$\omega_n=(n+\tfrac{1}{2}\beta')\Omega\pm\omega_L. \quad (2.14)$$

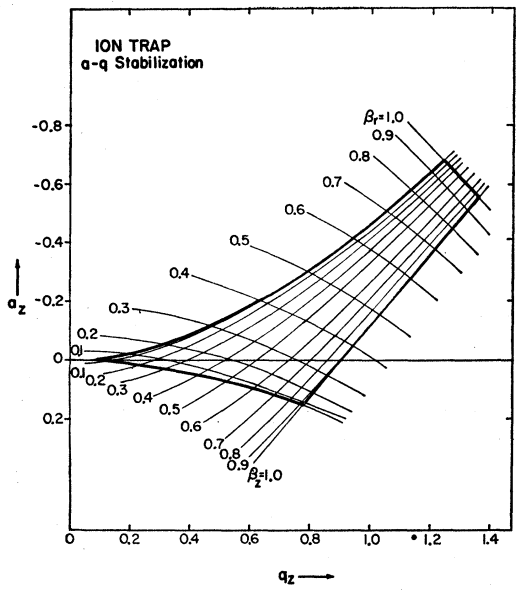

FIG. 2. Stability diagram in the a-q plane of the Mathieu equation for simultaneous confinement of ions in the r and z directions.

In the case of an atomic or molecular ion in relatively weak magnetic fields where $\omega_L/\Omega\ll 1$, the effect on the motion of the ions is small and uninteresting. However, for electrons the presence of a comparable magnetic field would have a dominant effect on their motion, and in fact, considerable experimental simplicity is achieved by confining them with the Penning gauge configuration.

The operating conditions of the trap are often such as to permit a useful approximation to be made in the description of the ion motion. Thus, if $a\ll 1$, $q\ll 1$, the following adiabaticity conditions may readily be verified to hold, except at the origin:

$$\rho\ll L, \quad R\ll L. \quad (2.15)$$

Here ρ is the amplitude of oscillation at frequency Ω, R is the mean distance traversed during the time $2\pi/\Omega$, and L is the distance over which the field amplitude changes by an appreciable fraction of itself. Under these conditions, as has been shown by several authors,[12] we may describe the motion averaged over a field period, i.e., the secular motion, as follows: Define the secular variables $\bar{x}$, $\bar{y}$, $\bar{z}$ by $x=\bar{x}+\xi$, where

$$\xi=-(e/m\Omega^2)E_x\cos\Omega t+\text{higher terms}, \quad (2.16)$$

and similar equations for the other coordinates. Then the motion is governed, to terms containing Ω^{-2}, by the following effective scalar potential field:

$$\psi=-(eE^2/4m\Omega^2)+\phi_0. \quad (2.17)$$

[12] See, for example, H. A. H. Boot, S. A. Self, and R. B. R-Shersby-Harvie, J. Electron. Control 4, 434 (1958); Ya. M. Pinskii, Zh. Tekhn. Fiz. 33, 864 (1963) [English transl.: Soviet Phys.—Tech. Phys. 8, 648 (1964)].

Here E is the amplitude of the rf component of the field, and ϕ_0 is the static component of the potential at $\bar{x}, \bar{y}, \bar{z}$. In the case of the quadrupole field, one sees that the secular motion is simple harmonic along any given coordinate axis. The frequency which may be identified with ω_0 is given by

$$\omega_0^2=\tfrac{1}{4}(a+\tfrac{1}{2}q^2)\Omega^2, \tag{2.18}$$

from which it follows that $\beta^2=a+\frac{1}{2}q^2$, a relationship used earlier.

On the basis of the adiabatic approximation, an important result concerning the energy of the ions becomes clearly evident. All ions with average energy less than some value $\bar{W}$ move within a region whose boundary is $e\psi=\bar{W}$, i.e., the ellipsoid

$$\beta_r^2r^2+\beta_z^2z^2=8\bar{W}/m\Omega^2. \tag{2.19}$$

The maximum energy which an ion may have and still be confined within the space defined by the electrodes will, in the absence of collisions, be that corresponding to the trap dimensions r_0 and z_0 as the amplitudes of oscillation for the r and z directions. However, this is unrealistic since collisions play an important role, as shown in the next section. An important corrollary is that ions introduced with a finite energy from outside the trapping region will not in the absence of collisions be confined within the trap.

III. EFFECT OF COLLISIONS

A. Background Atoms Unpolarized

Ideally, an ion pursuing a stable orbit within the trap will continue to do so indefinitely. However, in an actual system an ion may be expected to suffer collisions with other ions and neutral background particles in the trap. Since the ion densities are, in practice, small compared with those of background particles, ion-ion collisions will henceforth be neglected. Of the background particles, in the present form of the experiment there will inevitably be the parent atom or molecule with which the ion will undergo resonant charge-transfer collisions. There will also be the auxiliary reactant atoms introduced for their spin-dependent interaction with the ions, and, lastly, residual particles in the vacuum system. Of primary interest, of course, is the spin-dependence aspect of the problem, which will be dealt with separately later. However, the presence of collisions does profoundly affect the evolution of the energy distribution of the ions. Hence, for a given creation rate and maximum energy for ions which may be confined, both the total number of trapped ions and their lifetime in the trap are strongly affected. These two quantities are of primary interest in the further application of the trapping device and a full understanding of its limitations in respect to these quantities would indeed be desirable. However, in the present form of the technique it proved unnecessary to attempt[13] the solution of a difficult statistical problem which a realistic model would present. It will be sufficient to shed some light on the broad aspects of the problem.

One fundamental result concerning the energy of the ions can be stated immediately. Since collisions will continually redistribute the kinetic energy among the three translational degrees of freedom, the maximum energy $\bar{W}$ which a confined ion may have is not the value given in the previous section for the collision-free case, but is determined by the largest energy ellipsoid which can be described within the space defined by the electrodes, i.e., the smaller of $e\psi(r_0)$ and $e\psi(z_0)$.

Next we examine on the basis of the adiabatic approximation the effect of purely elastic collisions on the mean energy of a given ion. We ignore the higher moments of the distribution in the change of energy of an ion resulting from a collision at different phases of its motion which would be necessary for a complete description of the diffusion problem. Of particular interest is the dependence of the time behavior of the mean energy on the mass of the background particles. Consider ions of mass m undergoing purely elastic collisions with particles of mass m_r initially at rest in a rf field. The change in the energy of an ion per collision averaged over the phase of the rf field is shown in Appendix A to be, under certain conditions, given by

$$\langle\Delta\bar{W}\rangle_{\rm av}=m(1-\cos\theta)[m_r(m+m_r)^{-1}\langle v^2\rangle_{\rm av} -mm_r(m+m_r)^{-2}\langle u^2+v^2\rangle_{\rm av}], \tag{3.1}$$

where θ is the scattering angle, and u, v are the velocities of the secular motion and micromotion, respectively. It is convenient to consider separately the limiting cases $m/m_r\ll1$, $m/m_r\gg1$ and the important special case $m/m_r=1$.

In the first case, where $m/m_r\ll1$, the elastic collisions of the ions with what may be regarded as fixed scattering centers will lead to rf heating as in the familiar case of electrons, for which the statistical theory has been dealt with extensively in the literature. The essential physical ideas are brought out by considering the following simple model without the use of (3.1). Assume that the ions undergo purely elastic, totally randomizing collisions at intervals T_r with a "forest" of uniformly distributed fixed scattering centers in a uniform rf field. The c.m. of an ensemble of ions, all of which have just undergone a collision, will then be at rest at this instant t_1. Interaction with the rf field will, according to Eq. (2.16), cause the c.m. to move with a translational velocity $\mathbf{u}=-\mathbf{v}(t_1)$, on which, of course, the micromotion $\mathbf{v}$ is superposed. The average total energy of the c.m. motion, which is available for degradation into heat of amount $\Delta\bar{W}$ in the following randomizing collisions, is consequently per ion

$$\Delta\bar{W}=2(\tfrac{1}{2}m)\langle v^2\rangle_{\rm av}=2e\psi(\bar{\mathbf{r}}). \tag{3.2}$$

[13] D. C. Burnham, doctoral thesis, Harvard University, 1966 (unpublished).

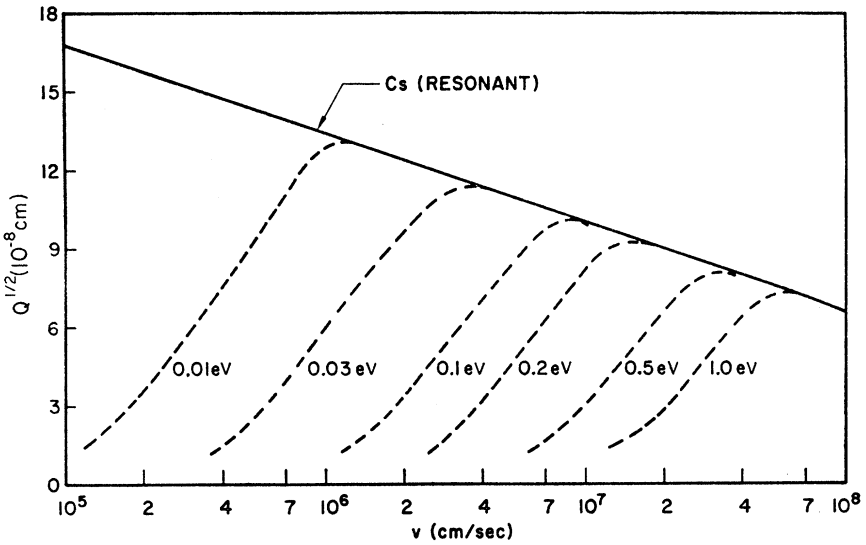

FIG. 3. Theoretical curves of Rapp and Francis (Ref. 18) for charge-exchange cross section Q as a function of the relative velocity in near-resonant collisions involving Cs, with the energy defect ΔE, as the single essential parameter.

If this is further averaged over the secular oscillation in a quardupole field, one has

$$\Delta\bar{W}=\bar{W}_0, \tag{3.3}$$

where $\bar{W}_0$ is the initial ion energy averaged over a period $2\pi/\Omega$. For a well-defined mean collision time T_r, this implies through the equation

$$\partial\bar{W}/\partial t=(1/T_r)\bar{W} \tag{3.4}$$

a purely exponential energy increase with time.

In the converse limit of $m/m_r\gg1$, where, as before, the background particles may be assumed to be relatively cold, collisions will essentially result in viscous drag which lowers the mean kinetic energy of the ions as a function of time. In this case the micromotion is not interrupted by the collisions, but only slightly modified in phase and amplitude, while any secular motion is damped out exponentially. This effect was first demonstrated experimentally for metallic particles in air[14] and later for Hg^+ in helium gas at about 10^{-5} Torr.[15]

In general, for arbitrary m/m_r, one may assume that Eq. (3.4) may be generalized ro read

$$\frac{\partial\bar{W}}{\partial t}=\alpha(m/m_r)\frac{\bar{W}}{T_r}, \tag{3.5}$$

where $\alpha(m/m_r)$ is a factor which is a function of m/m_r, having the value of approximately unity for small m/m_r and decreasing—ultimately becoming negative—as m/m_r increases. This raises the interesting question of what value makes $\alpha=0$. Here a hint is given in Eq. (3.1), for on setting $m=m_r$, it predicts zero change in the energy of a given ion when an average is taken over the secular oscillation. It is clear that this must be so in the special cases of head-on collisions and in the physically important resonant charge-exchange collisions between the ions and the parent atom, where charge exchange can occur with little momentum transfer.[16] In these cases the collision of an ion having initial energy $\bar{W}_0$ with a particle initially at rest results in the ion being at rest immediately after the collision. The subsequent absorption of energy from the rf field when averaged over the secular motion will again be $\bar{W}_0$, yielding a zero net increase in the ion energy.

It has been assumed in the foregoing discussion that the collision processes can be described in terms of a constant mean collision time. This is a fair approximation in general since the *average* total kinetic energy, as stated in (2.9), is independent of the time, and, moreover, to the extent that the interaction can be described by the monopole–induced-dipole inverse fourth-power law,[17] the assumption is rigorous. However, on the basis of experimental data, for example, for He^+-He at relative velocities exceeding about 10^6 cm/sec, the charge-exchange rate T_{ce}^{-1} becomes roughly velocity proportional.[18] The effect of this is that there will be a net increase in the ion energy, and the factor α will assume a small positive value. This is evident, in that, as the ion cloud regenerates itself through charge exchange with particles of zero velocity, it does this preferentially, where $\mathbf{c}=\mathbf{u}+\mathbf{v}$ is largest, which is in the region of large secular displacement where, according to Eq. (3.2), there is a positive increase in the energy.

Charge exchange with other atomic species leads, of course, to immediate loss of the ion of interest. The ions so formed could, by a proper choice of the operat-

[14] R. F. Wuerker, H. Shelton, and R. V. Langmuir, J. Appl. Phys. **30**, 342 (1959).
[15] G. R. Hugget and S. Menasian (private communication).
[16] W. H. Cramer and J. H. Simons, J. Chem. Phys. **26**, 1272 (1957).
[17] D. P. Stevenson and G. Gioumousis, J. Chem. Phys. **29**, 294 (1958).
[18] D. Rapp and W. E. Francis, J. Chem. Phys. **37**, 2631 (1962).

ing conditions of the trap, be in many cases trapped simultaneously—a circumstance which may be useful in the general application of the present technique.[19] The practical difficulty of achieving simultaneous confinement naturally increases with the disparity of the masses of the different species of ions.

B. Background Atoms Polarized: The He^+-Cs System

In this subsection, the equations of evolution of the populations of the various magnetic substates of the He^+ ion are derived for an ensemble of such ions undergoing spin exchange and spin-dependent charge exchange with Cs atoms having an electron spin polarization. The choice of Cs was originally made on the basis of the expected large spin dependence due to the different energy defects of different spin states for the charge-exchange reactions proceeding slowly along the triplet channels,

$$\mathrm{Cs}\uparrow + \mathrm{He}^+\uparrow \rightarrow \mathrm{He}^*(\uparrow\uparrow) \quad + \mathrm{Cs}^+ + \Delta E_3,$$
$$\mathrm{Cs}\uparrow + \mathrm{He}^+\downarrow \rightarrow \mathrm{He}^*(\uparrow\downarrow + \downarrow\uparrow) + \mathrm{Cs}^+ + \Delta E_3,$$

and fast along the singlet channel,

$$\mathrm{Cs}\uparrow + \mathrm{He}^+\downarrow \rightarrow \mathrm{He}^*(\uparrow\downarrow - \downarrow\uparrow) + \mathrm{Cs}^+ + \Delta E_1,$$

which are required to detect the ion spin polarization, acquired through spin exchange. The theory of Rapp and Francis[18,20] applied to the charge-exchange cross section Q for a nearly resonant reaction of the type $X^+ + A \rightarrow X^* + A^+ + \Delta E$, where the ionization energy I of the ground-state atom A and that of the excited-state atom X^* are nearly the same, is in agreement with this expectation. These authors find that Q can be approximated by a universal function

$$Q = Q(v, \Delta E, I) \tag{3.6}$$

containing only I, the energy defect ΔE, and the relative velocity v as parameters, independent of any other properties of the reactants. A family of Q curves, reproduced in Fig. 3, shows the strong dependence of Q on ΔE for low v values. The He levels $2s\,^1S$ and $2p\,^3P$ have the two smallest energy defects, $\Delta E_1 = 0.1$ eV, the closest accidental resonance with an alkali atom, and $\Delta E_3 = -0.25$ eV. At the velocity of interest, $v(\mathrm{He}^+\text{-Cs}) \simeq v(\mathrm{He}^+) = 1.7\times10^6$ cm/sec, one finds the very different corresponding cross sections $Q_1 \approx 6\times10^{-16}$ cm^2 and $Q_3 \approx 3\times10^{-17}$ cm^2. No correction for the higher statistical weight of the ^3P state has been applied, since, analogous to covalent chemical binding, only a single p orbital—the p_z orbital directed along the internuclear axis—is important. A lower limit for Q_e, the spin-exchange cross section, may also be obtained from the same graph by assuming $Q_e \gtrsim Q(\Delta E = 0)$. This yields $Q_e \gtrsim 170\times10^{-16}$ cm^2.

Allowing, then, that the cross sections for charge exchange for the He^+-Cs system exhibit a significant spin dependence, the problem remains of describing the time dependence of the state of an ensemble of He^+ ions and predicting the effect of induced rf transitions between the magnetic substates of the ions on their observed population decay. The ordering of the cross sections $Q_e \gg Q_1 \gg Q_3$ and the neglect of phase coherence between the states of the ions allows considerable simplification in the treatment of the problem and will be taken advantage of here; however, a more general treatment based on the density-matrix formalism is given in Appendix B.

Since the spin-exchange cross section is much larger than that for charge exchange, we may expect that in the absence of other perturbations, the electron spin polarizations, defined as $\langle s_z\rangle/s$, and denoted by p for the ions and P for the atoms, will be nearly equal, independent of the presence of nuclear spin on either collision partner.

A charge-exchange collision of a He^+ ion with a Cs atom in the $m_s = +\frac{1}{2}$ state may be considered as an "observation" of the He^+-ion spin state just as if an atom were traversing a Stern-Gerlach magnet, which can only give the result $m_s = +\frac{1}{2}$ or $m_s = -\frac{1}{2}$ for the atom. The angular splitting of the atomic beam in the Stern-Gerlach experiment is here replaced by a difference in the ion loss rate for ions with spins parallel and antiparallel to that of the atoms. To relate these ion loss rates, which may be denoted ν_p and ν_a, respectively, to the cross sections Q_1 and Q_3 introduced earlier, we note firstly that parallel spins correspond to a pure triplet state, while the wave function for the antiparallel case must, according to $\uparrow\downarrow = \frac{1}{2}(\uparrow\downarrow + \downarrow\uparrow) + \frac{1}{2}(\uparrow\downarrow - \downarrow\uparrow)$, be transformed into equal parts of triplet and singlet states. Assuming nearly identical translational orbitals for these states, it must follow that $\nu_p \propto Q_3$ and $\nu_a \propto \frac{1}{2}(Q_1 + Q_3)$. Also, for an ion sample of n ions, a description in terms of spin-state populations is readily obtained for ions having a spin polarization p interacting with atoms of polarization $P \neq p$, on recalling that the fractions of the ions having $m_s = +\frac{1}{2}$ and $m_s = -\frac{1}{2}$, which may be denoted n_+/n and n_-/n,

[19] Thus, for example, there may be advantages in some cases in measuring the number of atomic ions produced from the polarizing atomic beam through interaction with the ions under study.

[20] Compare also recent measurements on He^+-Cs charge exchange by Lorents and Peterson, which appear to be in agreement with this theory. D. C. Lorents and T. R. Peterson, in *Fourth International Conference on the Physics of Electronic and Atomic Collisions* (Science Bookcrafters, Inc., Hastings-on-Hudson, N. Y., 1965), p. 328; Phys. Rev. (to be published). Also, by now the analogous near-resonant reaction $H^+ + Cs \rightarrow Cs^+ + H^*(2s)$ has been exploited for the copious production of metastable H atoms: B. L. Donally, Phys. Rev. Letters **12**, 502 (1964). It is of course implied here that the near-resonant reaction channel exhibits the largest cross section. Along all other energetically possible channels, reactions will occur also, though generally with much smaller cross sections. In any case the over-all charge-exchange process will always exhibit some spin dependence. The extreme resonance of the competing, though generally not very likely, two-electron reaction $Cs + He^+ \rightarrow (Cs^+)^* + He$, for which energy defects as small as 0.008 eV can be found, does throw some doubt on the undisputed dominance of the one-electron channel leading to $Cs^+ + He^*$ assumed in the following.

are given by

$$n_+=\tfrac{1}{2}(1+p)n\,,\quad n_-=\tfrac{1}{2}(1-p)n\,. \tag{3.7}$$

Similar equations hold for N_+, N_- of the N atoms. Now the rate equations for these population numbers are given by

$$\begin{aligned} N\dot{n}_+&=-n_+N_+v_p-n_+N_-v_\alpha\,,\\ N\dot{n}_-&=-n_-N_-v_p-n_-N_+v_\alpha\,. \end{aligned} \tag{3.8}$$

Rewriting the population numbers in terms of the spin polarizations p, P, one finds, on adding the two equations,

$$-dn/dt=(n/T_0)[1-pP(\Delta Q/\bar{Q})]\,, \tag{3.9}$$

where $T_0^{-1}=\frac{1}{2}(v_p+v_\alpha)$, $\bar{Q}=\frac{1}{4}(Q_1+3Q_3)$, and $\Delta Q=Q_1-Q_3$. This analysis remains valid if Q_1, Q_3 are interpreted to refer to ion loss from *all* experimentally important processes, not only charge exchange. The polarization signal $S(pP)$ may now be defined as

$$S(pP)=[n(pP)-n(0)]/n(0)\,, \tag{3.10}$$

where $n(pP)$ and $n(0)$ refer to the number of ions remaining in the trap after an interaction time t_i. One may now adjust t_i to optimize the signal-to-noise ratio, assuming the Poisson fluctuations $n^{1/2}(0)$ of the ion number to be the only important noise source. Maximizing $S(pP)n^{1/2}(0)$ as a function of time yields for the optimum signal $S^*(pP)$

$$S^*(pP)=\tfrac{1}{2}pP(\Delta Q/\bar{Q})\,,\quad S^*\ll 1 \tag{3.11}$$

for $t_i=2T_0$. This result is a very useful relationship which is already applicable to such cases of interest as transitions between the magnetic substates of $(He^4)^+$ and the double-quantum transition between the $(1, +1)$ and $(1, -1)$ hfs levels of the $(He^3)^+$ ion. In such experiments, when using intense rf, one obtains $p=0$ and the vanishing of the signal. Without rf, a signal S^* corresponding to $p=P$ is observed. [See the center resonance of Fig. 9(b).]

In general, when discussing how transitions between the hfs levels of the ion affect the polarization signal, it is clearly sufficient, within the approximations of the present treatment, to consider only how these transitions affect the electron spin polarization p. This quantity may be expressed in terms of the population numbers n_α, n_β, n_γ, n_δ, adding up to n for the hfs states of the $(He^3)^+$ ion, $\alpha=(1, +1)$, $\beta=(1,0)$, $\gamma=(1, -1)$, $\delta=(0,0)$, and the electron spin polarization values, for which a look at the expanded wave functions shows

$$p_\alpha=+1\,,\quad p_\beta=0\,,\quad p_\gamma=-1\,,\quad p_\delta=0\,, \tag{3.12}$$

leading to

$$p=(p_\alpha n_\alpha+p_\beta n_\beta+p_\gamma n_\gamma+p_\delta n_\delta)/n=(n_\alpha-n_\gamma)/n\,. \tag{3.13}$$

In the absence of rf transitions and on the basis of the assumed ordering of the cross sections, neglecting at this point the relatively slow ion loss processes, the following rate equations may be obtained for the population numbers:

$$\begin{aligned} \dot{n}_\alpha&=-2(1-P)n_\alpha+(1+P)n_\beta &&+(1+P)n_\delta\,,\\ \dot{n}_\beta&=\ (1-P)n_\alpha &&-3n_\beta+\ (1+P)n_\gamma &&+n_\delta\,,\\ \dot{n}_\gamma&= &&(1-P)n_\beta-2(1+P)n_\gamma+(1-P)n_\delta\,,\\ \dot{n}_\delta&=\ (1-P)n_\alpha &&+n_\beta+\ (1+P)n_\gamma &&-3n_\delta\,. \end{aligned} \tag{3.14}$$

This result may be arrived at in an elementary way (allowing some insight into the spin-exchange process) which will be outlined in the following.

During the spin-exchange collision in which electronic angular momentum is transferred to the He^3 ions, the nuclei are not immediately affected. Nevertheless, in the long collision free interval afterwards, the hfs precession in the He^3 ion does transfer angular momentum from the electron to the He^3 nucleus. Since the collision frequency T_p^{-1} of a He^+ ion with Cs atoms is largely determined by the spin-independent polarization forces, we schematize the collision process as follows. At average intervals T_p, the exchange interaction between pairs of fixed He^+ ions and Cs atoms is switched on for a statistically varying time, long compared with the spin-exchange period. During the interaction period, the $(He^3)^+$ nuclear wave functions remain unchanged, while the electron spin wave functions evolve in time because they are a superposition of two stationary states, singlet and triplet, with different energies.[21] Thus, for example, an initial wave function $\Psi_i\propto\uparrow\beta$ must be written

$$\Psi_i\propto 2\uparrow\uparrow\downarrow+[(\uparrow\downarrow+\downarrow\uparrow)+e^{i\Phi}(\uparrow\downarrow-\downarrow\uparrow)]_{\Phi=0}\uparrow\,, \tag{3.15}$$

where

$$\Phi=-(E_3-E_1)t/\hbar\,.$$

In the term $2\uparrow\uparrow\downarrow$ the first two arrows refer to the electronic spins of Cs and $(He^3)^+$, while the third denotes the nuclear spin of the He ion. An analogous position convention is used in the following. After a time t this becomes, after bracketing out the Cs electron spin function,

$$\Psi_f\propto\uparrow[2\uparrow\downarrow+\downarrow\uparrow(1+e^{i\Phi})]+\downarrow[\uparrow\uparrow(1-e^{i\Phi})]\,. \tag{3.16}$$

Transforming back to the coupled representation for the $(He^3)^+$ ion, we find

$$\Psi_f\propto\downarrow[\sqrt{2}(1-e^{i\Phi})\alpha]+\uparrow[(3+e^{i\Phi})\beta+(1-e^{i\Phi})\delta]\,. \tag{3.17}$$

The effect of the hfs interaction which we now switch on is to multiply δ in this expression by $e^{i\Phi_{hfs}}$, quite analogous to the procedure leading to (3.15). However, this phase factor has no effect on the average populations in the states α, β, γ which we obtain by averaging the squares of the absolute values of the expansion coefficients in (3.17) over Φ. We see that as a result of the collision, an ion initially in the $\uparrow\beta$ state has the relative probabilities $\frac{1}{4}$, $\frac{5}{8}$, and $\frac{1}{8}$ of appearing afterwards

[21] E. M. Purcell and G. B. Field, Astrophys. J. **124**, 542 (1956).

TABLE I. Relative signal strength S' of saturated rf transitions between hfs levels of $(He^3)^+$.

Transition	$P \ll 1$	$P=1$
(1, +1)-(1, 0)	0.4	4/7
(1, +1)-(1, −1)	1.0	1.0
(1, 0)-(1, −1)	0.4	0.0
(1, +1)-(0, 0)	0.4	4/7
(1, 0)-(0, 0)	0.0	0.0
(1, −1)-(0, 0)	0.4	0.0

in the α, β, δ states, respectively. An analogous procedure is applicable to the other $(He^3)^+$-ion hfs states and the rates at which ions in an ensemble are scattered in and out of the hfs levels for a general Cs spin polarization P can be written down using the $\frac{1}{2}(1+P)$ and $\frac{1}{2}(1-P)$ weighing factors for the two Cs electron spin states. In this way the system of Eq. (3.14) may be constructed. It should be noted that, as defined, T_p is the mean time between collisions which randomize Φ and for which the probability of spin exchange is only $\frac{1}{2}$. Since Q_e is defined in terms of a mutual spin flip, the corresponding T_e must be related to T_p by $T_e=2T_p$. For simplicity of appearance, Eqs. (3.14) have been written with the time measured in units of $4T_e$.

To demonstrate the usefulness of these equations, we derive the relative signal strength for saturated rf transitions between the hfs levels, e.g., α and β, under slow passage conditions. Since $S \propto p$ and $p=P$ in the absence of rf transitions, we define the corresponding relative depolarization signal as

$$S_{\alpha\beta}' \equiv 1-(p_{\alpha\beta}/P) = [n(PP)-n(p_{\alpha\beta}P)]/[n(PP)-n(0)]. \quad (3.18)$$

The transition reduced ion polarization $p_{\alpha\beta}$ is found from Eq. (3.13) and the solution of the rate equations in (3.14) for $\dot{n}_\gamma$, $\dot{n}_\delta$ under the conditions $n_\alpha=n_\beta$ and $\dot{n}_\gamma=\dot{n}_\delta=0$. The numerical results for the signals $S_{\alpha\beta}$ for the limiting cases $P\ll 1$ and $P=1$ are listed in Table I and formulas (6.1) are applicable for general P. The equilibrium value $p=P$ postulated earlier also follows easily from (3.14).

IV. DETECTION OF CONFINED IONS

On the basis of the foregoing section, the problem of analyzing the spin polarization of a trapped ensemble of ions may be reduced to that of precisely monitoring their lifetime against loss due to scattering from polarized atoms. This presupposes that the number of ions remaining after a precisely determined interval can be measured without undue difficulty. It is therefore of fundamental importance to the present technique to examine the methods by which this may be accomplished.

In principle, the simplest and therefore the best method is to accelerate the ions out of the trap and count them with an electron multiplier[22] or measure their integrated current; and for studies involving a wide variation of parameters, such an absolute method is essential. However, since we were interested only in observing small relative changes in the ion number, it was possible to use a method which is considerably simpler in practice, namely, the method of rf resonance absorption of Paul *et al.*[11,23] As already pointed out in Sec. II, the ion motion in the rf quadrupole trap has a discrete frequency spectrum, which has the component $\omega_0=\frac{1}{2}\beta\Omega$ corresponding to $n=0$. This circumstance permits the detection of the ions by the resonance excitation of this mode along the z axis by a weak rf dipole field, applied for this purpose from a high impedance source, which in practice takes the form of a high-Q parallel L-C circuit, as shown in Fig. 1. This tank circuit is coupled capacitatively with the oscillating electric-dipole moment of the ion cloud in the trap in close analogy with the inductive coupling of nuclear moments in NMR. To bring out this analogy more explicitly, consider an ensemble of n_0 ions, initially with a uniform distribution of amplitudes and phases, moving under the influence of a uniform detection field of frequency ω, in the neighborhood of their characteristic frequency ω_0. We neglect the higher-frequency components in the ion spectrum, and also collisions, since the collision probability is small during the time of observation. Then the vector amplitude of the motion of the center of charge Z_c, defined by $z_c=Z_c(t)e^{i\omega t}$, will in the neighborhood of resonance obey an equation of the form (see Appendix C)

$$[1+(k^2/4\omega^2)]\dot{Z}_c+\{(\tfrac{1}{2}k)[1-(\Delta/\omega)]+i[(k^2/4\omega)+\Delta]\}Z_c = -(i\gamma/2\omega)[1+(ik/2\omega)], \quad (4.1)$$

where $\Delta=\omega-\omega_0$, $\gamma=eE/m$, E being the amplitude of the detection field, and $k=(n_0e^2Q)/(4m\omega z_0^2C)$. This is essentially the form taken by the equation for $u+iv$, the vector amplitude of the transverse magnetization in the Bloch equations of NMR as applied in a paper by Jacobsohn and Wangness[24] to the question of line shape at finite sweep rates. Under the conditions of interest here the damping factor k is negligible, and hence, for a linear frequency sweep, $\Delta=at$, the solution of Eq. (4.1) is expressible in terms of the Fresnel integrals.[24]

A dominant characteristic of this method of ion detection not present in the NMR case is the neutralization of ions brought into contact with the electrodes as a result of their excitation by the detection field. This will, of course, significantly affect the line shape and sets an upper limit on the amplitude of the motion of the ions, and hence, for a given initial ion number, the size of the signal observed. Thus, under the con-

[22] K. B. Jefferts, Phys. Rev. Letters **20**, 39 (1968).
[23] G. Rettinghaus, doctoral dissertation, University of Bonn, 1965 (unpublished); Z. Angew. Phys. **22**, 321 (1967).
[24] B. A. Jacobsohn and R. K. Wangness, Phys. Rev. **73**, 942 (1948).

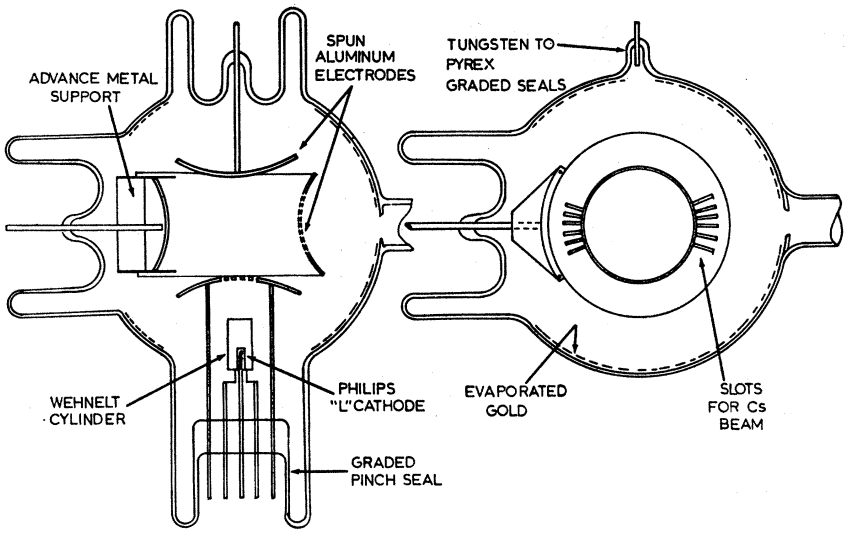

FIG. 4. Constructional details of the quadrupole-ion cage assembly.

ditions assumed above, the maximum signal voltage appearing on the tank circuit, whose resistance at resonance is $R_r=Q/\omega C$, may be estimated as

$$e_{\max}\approx(R_r n_0 e/2z_0)(\dot{z}_c)_{z_c=\frac{1}{2}z_0}=n_0 eQ/4C. \qquad (4.2)$$

Now the ultimate sensitivity is limited ideally by the thermal noise in the resistance R_r, which in a bandwidth $\Delta\nu$ has the RMS value $e_n=(4kTR_r\Delta\nu)^{1/2}$. For the typical practical values $C=100$ $\mu\mu$F, $Q=200$, $\omega=10^6$ rad/sec, $\Delta\nu=100$ Hz,[25] this sensitivity is on the order of 10^2 ions. However, it is not the sensitivity that was of primary concern in the He^+-ion experiment, but rather the optimum signal-to-noise ratio for a given sufficiently large number of ions, a ratio fundamentally limited by the shot ion noise.

The interpretation of the ion resonance signal as a measure of the ion number must be made with caution. Under actual conditions, the detection process is complicated by two important circumstances: Firstly, the actual trap will inevitably have some anharmonicity, the frequency either increasing or decreasing with amplitude depending on the actual geometry of the electrodes, and this can lead to a complicated interaction of the ions with the driving field[26]; secondly, the detection field as applied in practice is necessarily nonuniform, and higher-order moments in the ion charge distribution may be excited. The effect of the latter is that, in contrast with the uniform-field case (where the signal is due solely to the motion of the center of charge, and hence is unaffected by the Coulomb interaction between the ions themselves), a dependence of the observed line shape on the ion number will result.

V. APPARATUS

A. Ion Trap

The entire vacuum system was constructed out of Pyrex glass with all leads to internal electrodes made through graded seals as shown in Fig. 4. The electrodes were spun out of pure-grade aluminum, baked in air to remove imbedded wax used in the spinning operation, then thoroughly cleaned chemically, and finally, a thin layer of pure silver was evaporated onto the inner surfaces. Small brackets of a more resistive metal were rivetted to the electrodes and served to support them by spot welding to their tungsten leads. The heavy tungsten rod supporting the cylindrical electrode also served to provide a thermal connection to a dry-ice bath to insure efficient condensation of the Cs, and thus minimize the background of unpolarized atoms due to back scattering. Although this method of assembly is inherently less accurate than the use of precision spacers between the electrodes, it circumvents difficulties with electrical leakage caused by the formation of surface layers of Cs. The electrode dimensions were chosen as $z_0=2.5$ cm and $r_0^2=2z_0^2$.

Since the lifetime of the ions in the trap is limited by scattering with background particles, it is critically important that the density of the residual gas in the system be sufficiently small that the lifetime is long compared with the mean collision time with the Cs atoms. Since the mean density of polarized atoms averaged over the volume of the trap is experimentally limited to the order of 10^{+9} cm^{-3}, the above condition implies a background pressure not exceeding 10^{-8} Torr. Advances in ultrahigh vacuum technology, having just at that time received a great impetus through the development of the getter ion pump, prompted the initial

[25] The bandwidth may profitably be reduced to optimize the S/N ratio by reducing the sweep rate only up to a point determined by the phase-coherence time of the ions [see Richardson *et al.* (Ref. 10)].

[26] W. E. Lamb, Jr., in *Quantum Optics and Electronics*, edited by C. DeWitt, A. Blandin, and C. Cohen-Tannoudji (Gordon and Breach Science Publishers, Inc., New York, 1965), p. 338.

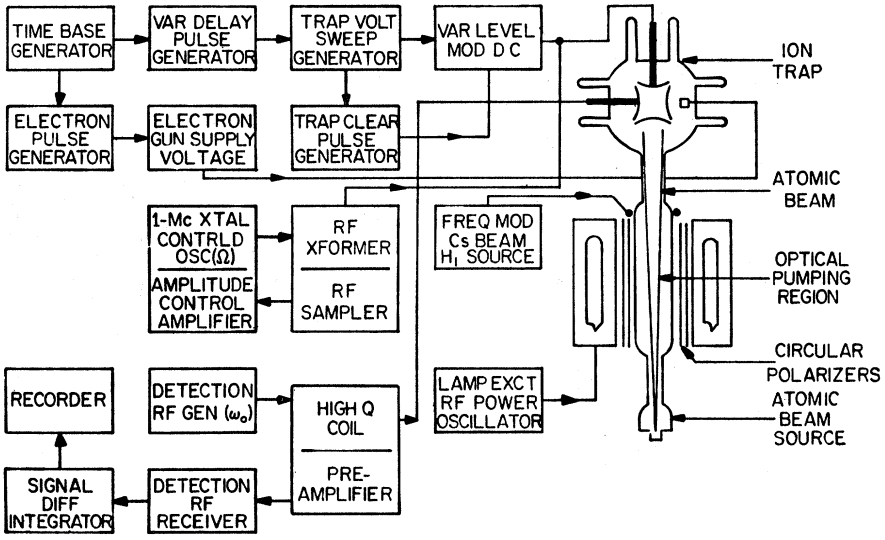

FIG. 5. Block diagram of apparatus for observation of orientation and magnetic resonance of stored He^+ ions. A horizontal static magnetic field $H_0 \simeq 7$ G was applied by Helmholtz coils over the whole beam tube. Its direction was parallel to the plane of the drawing.

attempt of the present experiment. Two 15-liter/sec pumps were used, with their magnets arranged to form a quadrupole, and were connected to the system through a glass manifold of sufficient length to reduce the magnetic-field gradients at the site of the trap to a tolerable value. Pure He gas was introduced into the system through a quartz diffusion leak provided with a glass jacket, which could be pumped out if necessary to eliminate diffusion of the gas into the system at room temperature.

B. Electronics

The polarization dependence of the ion lifetime was displayed by a "time-bridge" method in which an identical number of ions are produced from the background He gas by a periodically gated electron beam, and the number of ions remaining near the end of consecutive interaction periods are compared as the polarization of the Cs atoms is destroyed for alternate periods. In order to achieve a signal-to-noise ratio approaching the theoretical limit determined by shot noise, it is necessary not only to have a sufficient stability in the intensity and duration of the electron beam, but also in the density of the He gas. Moreover, the amplitude and frequency of the trapping field and the physical parameters in the detection process must be rigidly stable. A block diagram of the electronics is shown in Fig. 5. All supply voltages including those for cathode heaters were electronically regulated. The source of the rf trapping voltage was a 1-Mc/sec crystal controlled oscillator with automatic ampltiude control capable of providing 100–300-V variable amplitude at the trap. The dc component of the trapping field was synthesized from a regulated dc voltage variable from -5 to $+15$ V and a negative going sawtooth of variable amplitude and duration derived from a precision waveform generator. This sawtooth was triggered by a variable delay pulse obtained from a pulse generator in conjunction with a master time-base generator. A -50-V clearing pulse obtained from a univibrator triggered by the fly-back of the dc sweep was incorporated to eliminate difficulties which may arise from the incomplete emptying of the trap by the detection field.

The electron gun, which consisted of a type-L Philips impregnated cathode mounted coaxially with a Wehnelt cylinder, was gated by applying a large positive pulse to the latter derived from a Schmidt trigger circuit activated by the master sawtooth generator. The cathode heater was run on a rf supply.

The trapping potentials were applied to the cylindrical electrode, the cap electrode near the electron gun being grounded "hard," while the other cap electrode carried the detection rf voltage. This latter electrode was connected through a high-L/C parallel L-C circuit, in the form of a low-capacitance winding on a ferrite core and a trimmer capacitor, to ground. To reduce the amplitude of the trapping rf voltage appearing on this same electrode, it was necessary to provide a high-Q series resonant L-C shunt filter to ground. The parallel L-C circuit tuned to the detection frequency had a measured Q approaching 200 at a frequency of 100 kc/sec, giving a shunt resistance at resonance of nearly 2.4 MΩ. The rf voltage appearing on this L-C circuit from a loosely coupled source of the detection rf was amplified by a two-stage tuned amplifier connected to the tank circuit through a cathode follower preamplifier. The amplified rf signal is then detected, filtered, and displayed on an oscilloscope whose horizontal deflection was driven by the sweep voltage of the ion frequency.

C. Source of Polarized Cs Atoms

Cs atoms issuing from a refluxing type of oven which was an integral part of the glass vacuum shell as shown

in Fig. 6, were given an electron spin polarization by optical pumping[27] over an approximate 30-cm length of their path to the ion trap. The source of the resonance pumping radiation were two specially constructed cylindrical Cs vapor lamps excited inductively by rf coils energized from a 8-MHz, 500-W power oscillator. Commercial sheet linear polarizers and retardation films were used to produce the circular polarization of the resonance light needed for the process of optical pumping. Of crucial importance to the achievement of high atomic polarization by this process is the condition that the profile of the emission lines from the lamps be as free as possible of self-reversal consistent with a high over-all brightness. This means that the surface temperature of the lamps and the temperature of the Cs metal must be carefully adjusted to obtain optimum conditions. This was achieved through a combination of surface air cooling and adjustment of the proximity of the metal reservoir to the intense region of the exciting rf field. The lamps were mounted in front of mirrors approximating elliptical cylinders, with horizontal collimators placed in front of the lamps to limit the angular spread of the pumping beam in the vertical plane. At the two extremities of the optical-pumping region of the tube, refrigeration coils were wound with the object of cooling the glass surfaces to about $-30°C$. A study of the vapor-pressure data for Cs reveals that at room temperature, the equilibrium vapor pressure is as high as 10^{-6} Torr, which corresponds to a density comparable with that in the atomic beam—an obviously intolerable situation. Fortunately, the vapor pressure falls approximately one decade per 20°C, and thus at $-20°C$ it is already of the order of 10^{-8} Torr. In addition to this method of reducing background Cs pressure, another was used consisting of providing free gold surfaces, with which, as previous experience had shown, the Cs readily amalgamates, reducing the equilibrium vapor pressure at room temperature to an extremely low value.

D. Magnetic Field

Unlike the atomic-beam technique for neutral particles in which strong magnetic fields are necessary and ferromagnetic materials are generally used, there is in the present experiment no process relying on the presence of high magnetic-field intensities, and ferromagnetic materials are in fact carefully avoided. Moreover, one of the primary aims of the experiment is to realize the narrow spectral linewidths made possible by the long observation times. Therefore the field should be sufficiently uniform about a low intensity value that the field-independent transition (1,0)-(0,0) in the $(He^3)^+$ ion is not appreciably broadened by residual field gradients.

[27] A. Kastler, Proc. Phys. Soc. (London) **A67**, 853 (1954). For calculations of optical pumping rates for ^{133}Cs, see W. B. Hawkins, Phys. Rev. **123**, 544 (1961), and more recently, P. Violino, Nuovo Cimento **45B**, 166 (1966).

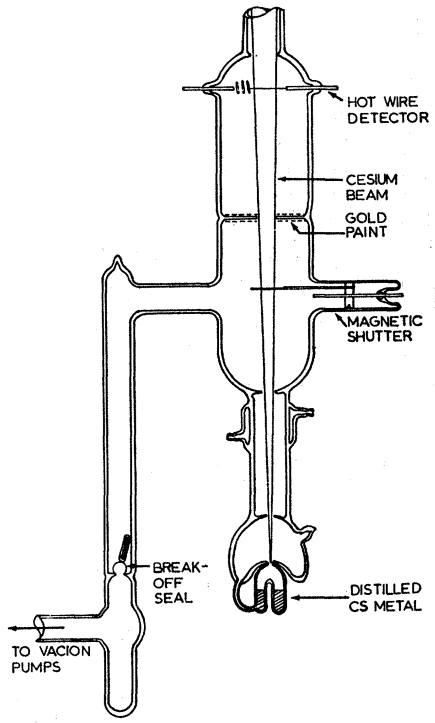

FIG. 6. Cs atomic-beam section of the glass vacuum system, showing the refluxing oven source. The two lower beam-defining apertures were kept hot by auxiliary heaters.

The primary source of magnetic field was a large (150-cm mean diameter) Helmholtz pair, wound in accordance with the Maxwell condition $(a/b)^2=36/31$, where a is the radial depth of winding and b the axial width. The coils, having 4680 turns each, were wound on surface water-cooled brass forms, with an Epoxy resin being used as filler between windings to improve the heat-transfer efficiency to the surfaces. The magnetic "efficiency" of the coils was approximately 56 G/A, with a theoretical inhomogeneity of 3 ppm over a 2.5-cm radius at their common center. The ion trap was positioned coaxial with these coils.

VI. RESULTS

Operating the trap with $U_0=7$ V, $V_0=175$ V, and $\Omega/2\pi=10^6$ Hz, which corresponds to $a_z=0.03$, $q_z=0.34$, yielded $\omega_0/2\pi=1.1\times10^5$ Hz. In the trap center, the maximum ion velocity may be expressed as $\omega_0 z_0$, which, with $z_0=2.5$ cm, has the value $\omega_0 z_0=1.73\times10^6$ cm/sec. This value was used to obtain the theoretical charge-exchange cross sections Q_1 and Q_3. The corresponding kinetic energy, and also the local maximum kinetic energy *averaged* over $2\pi/\Omega$ anywhere in the trap, are equal to $e\psi(z_0)=6.2$ eV, the trap depth. By contrast, the maximum *instantaneous* kinetic energy reached on the trap periphery was $2e\psi(z_0)=12.4$ eV. Since $r_0/z_0=\sqrt{2}$, the dc contribution to $\psi(z_0)$ was $\phi(z_0)=-3.5$ V $=-\phi(r_0)$. From this follows $\psi(r_0)=8.4$ V $>\psi(z_0)$.

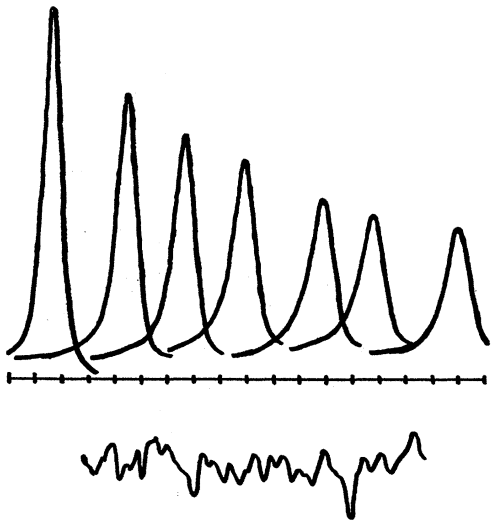

FIG. 7. Series of motional resonance signals indicating ion populations stored for increasing periods, showing the decay due to collisions with the background gas. Storage intervals were increased incrementally up to 10 sec. The individual resonances were traversed at a sweep rate of 30 divisions/sec, and the resulting patterns were shifted corresponding increments by adjusting the oscilloscope time-axis zero. Display bandwidth was 200 Hz. The lower trace corresponds to off-resonance noise when the gain was increased one-hundred-fold, demonstrating an initial signal-to-noise ratio of ~1000.

The ion-population resonance signal had a ratio to the baseline noise under optimum conditions of sweep rate and detection rf amplitude approaching $10^3:1$ (see Fig. 7). This is consistent with estimates $n_0 \simeq 10^7$ ions which were obtained by the procedures underlying formula (4.2). However, the fluctuation in the signal height over consecutive cycles was observed to be a factor of 10 greater than the baseline noise. Since the absolute signal height falls short of that necessary to make the results consistent with shot noise as the source of the fluctuation, it must be presumed to be due to instabilities in the many factors already mentioned which determine the signal height.

By varying the time delay between the formation of the ions and their detection, the mean lifetime of the ion population was determined (see Fig. 7). Firstly, the lifetime as determined by collisions with residual gas particles was measured, yielding approximately 8 sec for a pressure of about 3×10^{-8} Torr. When the Cs oven was brought up to the operating temperature of about 90°C and a comparison made between the lifetime with and without the Cs atoms traversing the trap by operating a beam shutter provided for this purpose, it was found that the presence of the Cs reduced the lifetime from 8 to 0.4 sec.

Since the ultimate polarization effect depends quadratically on the spin polarization of the Cs atoms, it is particularly important that this polarization not be degraded by the use of too great a density in the atomic beam, or improper operation of the lamps and circular polarizers. With the aid of an RCA 7102 photomultiplier which has a spectral response appropriate to the resonance D lines of Cs (8943 and 8521 Å), the fluorescence of the Cs beam was observed near the exit of the optical-pumping region. By periodically destroying the atomic polarization with a frequency-modulated H_1 field, a rough relative measure of the atomic polarization was obtained by observing the relative depth of modulation of the intensity of the fluorescence. Since an unfiltered mixture of both the D_1 and D_2 lines was detected, the dependence of the photomultiplier output on the atomic polarization is a strong function of the relative intensities of the two D lines. However, it should be a valid indication for the purpose of optimizing the atomic-beam intensity. A modulation amounting to roughly 30% was observed in the intensity of fluorescence up to a beam density corresponding to an oven temperature of 95°C. This was obtained with the lamps running under optimum conditions when the total light output as measured by a 2.5-cm-diam silicon solar cell placed 10 cm from a bare lamp yielded a short circuit photocurrent of 12 mA, corresponding to a surface brightness approaching 5×10^{16} photons cm^{-2} sec^{-1}.

The interaction time was set at 0.8 sec, that is, twice the observed time of 0.4 sec for the decay of the ion population, as demanded by the results of Sec. III. Then the integrated difference in the ion-population signal between consecutive cycles was monitored as the atomic spin polarization was reduced during alternate periods by the frequency-modulated H_1 field acting on the Cs atoms. It was observed that when the atomic polarization was fully modulated, the strength of the ion-population signal showed a 4% modulation. This indicated that indeed the ion lifetime is a function of the atomic polarization, and the ions themselves must have developed a spin polarization. The mean fluctuation in the ion signal for a fixed polarization was about 1%, which means that the polarization signal-to-noise ratio was 4 per observation. This was improved by an order of magnitude by integrating the difference

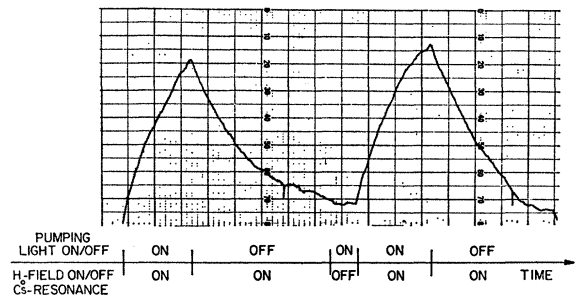

FIG. 8. He^+ polarization as demonstrated by pulse difference integrator output as function of Cs spin polarization. The Cs polarization was on-off modulated by a resonant rf field applied in the beam region during alternate interaction cycles. The essential element of the integrator was an R-C circuit with a 100-sec time constant into which alternate signals monitoring the residual ion charge were fed with opposite polarity. A division corresponds to about 30 sec.

of consecutive signals with a 100-sec time constant, as shown in Fig. 8. Here are also shown the various control experiments to verify the authenticity of the polarization effect. These experiments clearly showed that the effect was present if and only if both the pumping light was on and the frequency of the H_1 field for the modulation of the Cs spin polarization was tuned to a value appropriate to the applied H_0 field.

These original experiments were carried out on $(He^4)^+$ ions since, in contrast with the mass-3 isotope for which $I=\frac{1}{2}$, charge-exchange collisions with neutral He atoms leave the electron spin polarization of the ion ensemble unchanged. In the case of the $(He^3)^+$ ion, such collisions, which result, in effect, in a sudden exchange of the nuclei, provide a mechanism by which angular momentum is transferred to the nuclei of the background He atoms, at the expense of the ions. Hence the requirement on low-background He pressure is more stringent for He^3 than He^4. At a reduced base pressure approaching 10^{-9} Torr, the polarization effect was also observed for $(He^3)^+$ ions both by modulating the polarization of the Cs atoms, as was done for the $(He^4)^+$ ions, and also by the application of a frequency-modulated H_1 field acting on the ions to induce the low-frequency Zeeman transitions $\Delta F=0$, $\Delta m_F=\pm 1$. The H_1 field at a frequency near 10 MHz was applied by means of a one-turn loop, which surrounded the trap bulb and whose plane contained both trap and Helmholtz-coil axes.

The observed values of the relative signal strengths $S_{\alpha\beta}'$ and $S_{\beta\gamma}'$, which can readily be determined from Fig. 9(b), provide a sensitive measure of the Cs spin polarization attained in the experiment. Thus the solution for $p_{\alpha\beta}$, $p_{\beta\gamma}$ and hence $S_{\alpha\beta}'$, $S_{\beta\gamma}'$ obtained from the rate equations (3.14) may be inverted to yield

$$P=(5S_{\alpha\beta}'-2)/(2-2S_{\alpha\beta}'),\qquad P=(2-5S_{\beta\gamma}')/(2-2S_{\beta\gamma}'). \tag{6.1}$$

Substituting the approximate experimental values $S_{\alpha\beta}'=0.5$ and $S_{\beta\gamma}'=0.27$, one finds $P=0.5$ and $P=0.45$. This relatively high degree of Cs spin polarization is in agreement with the observation that a reduction of the pumping light intensity by a factor of 2, achieved by simply blocking the light of one of the two Cs lamps illuminating the beam, affected the signal S^* much less than the factor of 4 which would be expected from Eq. (3.11), if $P\ll 1$ and if P were in the region of linear dependence on pumping light intensity.

The experimental value $P=0.5$ deduced above may be used with the observed $S^*=0.04$ to give $\Delta Q/\bar{Q}\simeq 0.32$. This is an order of magnitude less than the theoretical value calculated from the purely charge-exchange values of Rapp and Francis, which we now denote by Q_1^{ce}, Q_3^{ce}. This suggests that considerable ion loss is due to rf heating associated with He^+-Cs spin-independent momentum-transfer collisions, as discussed in Sec. III A. Assigning an effective average cross section

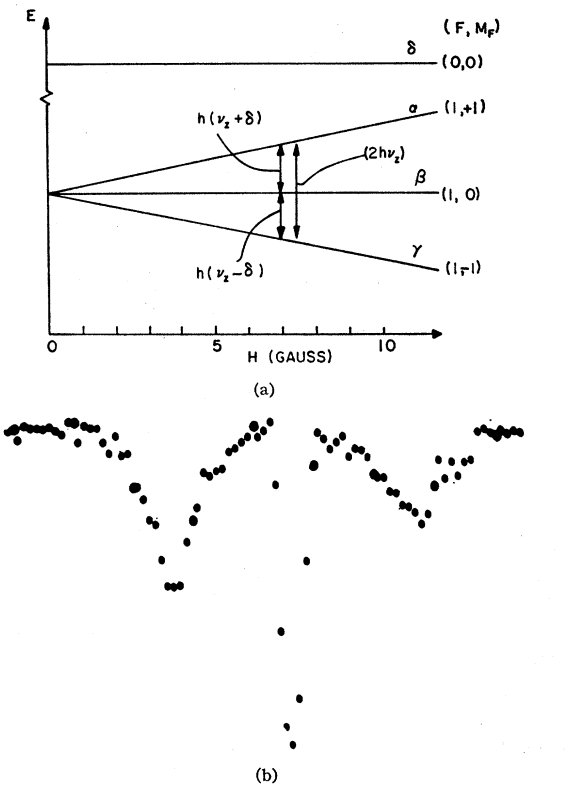

FIG. 9. (a) Low-field region of Breit-Rabi diagram for the hfs energy levels of $(He^3)^+$ as a function of magnetic field H. (b) Digital-analyzer display of the rf saturated $\Delta F=0$ spectrum of $(He^3)^+$ obtained with the Cs optically pumped into the $m_s=-\frac{1}{2}$ state resulting in a depolarization signal S' greater for the lower frequency (1, −1)-(1,0) transition than the (1,0)-(1, +1) transition. The relatively narrow line in the middle is the double quantum transition (1, −1)-(1, +1). The magnetic field had the value $H=7.23$ G, for which the spectrum was centered about 10.01 MHz, and the Paschen-Back-Goudsmit shift amounted to $\delta=11.5$ kHz. The frequency increases from left to right, and the quantity plotted is simply n(0.8 sec), the number of stored ions remaining after the interaction interval, averaged over 80 traversals of the spectrum with the zero strongly suppressed.

Q_i for this spin-independent loss process, we attempt to evaluate Q_i by substituting $Q_1^{ce}+Q_i$, $Q_3^{ce}+Q_i$ for Q_1 and Q_3 in Eq. (3.9). Then Eq. (3.11) takes the form $S^*=\frac{1}{2}P^2\Delta Q^{ce}/(\bar{Q}^{ce}+Q_i)$. On substituting the numerical values found experimentally for S^* and P, and the theoretical values of Q_1^{ce}, Q_3^{ce} due to Rapp and Francis, one obtains $Q_i\approx 10\bar{Q}^{ce}$. This suggests a wide potential margin for improvement in other experiments by using the lightest possible polarization carriers consistent with a strong spin dependence of the charge-exchange process or making use of a suitable ion-cooling mechanism.

VII. DISCUSSION

The results clearly show that a spin dependence in collision processes leading to the neutralization or loss (and by induction, the formation) of ions stored in an electrodynamic trap is observable through interaction with a beam of polarized particles. Rather than make

the object of further work the detailed study of such processes, our intention remained, as originally stated, to exploit these processes for the study of the rf spectrum of the $(He^3)^+$ ion as a first concrete example of a new general technique.

Since the signal-to-noise ratio attained in our polarization and the $\Delta F=0$ rf magnetic resonance experiments suggested that the $\Delta F=\pm 1$ spectrum should be observable, work was commenced to modify the apparatus for the provision of a microwave H_1 field in the ion trap to induce these transitions. This necessitated the rebuilding of the trap to approximate a cylindrical resonator operating in the TE_{013} mode, with a $\frac{1}{2}\lambda$ slot antenna, and mounting it with its axis approximately at 45° to the magnetic field in order to induce both σ and π transitions as desired. The work was taken up at this point and continued by Fortson in collaboration with one of the authors (H. G. D.). The digital-analyzer display of the $\Delta F=0$ transitions reproduced in Fig. 9(b) was obtained by Schuessler, using the modified apparatus. The $\Delta F=\pm 1$ spectrum has also been observed[2] now, and the work in progress on the detailed study of the $(He^3)^+$-ion rf spectrum will be the subject of a later publication.

The universal and dominant character of the spin-exchange process as a polarizing agent, which can compete with most disorienting side reactions conceivable, suggests that our ion storage-exchange collision technique should be further applicable to almost any, not only S-state, atomic or molecular ions with unpaired electron spin. This assumes that a sufficiently large relative spin dependence of the total cross section for ion loss, $\Delta Q/\bar{Q}$, can be realized to enable the detection of the ion-spin polarization. This requires a judicious choice of atoms in the polarized beam (alkali metals, H, etc.) and of ion energy in order to realize a sizeable charge-exchange cross section for one of the multiplet states (preferably the singlet) which substantially exceeds that of the other. Moreover, to minimize spin-independent ion loss, the lightest beam atom should be chosen compatible with the above, This should present no insurmountable problems. especially when beams totally polarized by magnetic-state selectors and suitably shaped ion-trap structures are used, and it is feasible to collect and obtain a measure of the number of beam atoms ionized in the exchange reaction, rather than that of the stored ions under study.

ACKNOWLEDGMENTS

We are indebted to Dr. E. N. Fortson and also Dr. Hans A. Schuessler for contributions to the later development of the technique; to David Church, Stephen Menasian, and Philip Ekstrom for their assistance in the running and designing of some of the $(He^3)^+$ equipment; and to Jake Jonson, whose expertise in the construction of the glass system greatly contributed to the success of the experiment. One of us (F. G. M.) would also like to express his gratitude for the hospitality shown him at the Physikalisches Institut, Universitaet Bonn, where portions of the manuscript were prepared. We should also like to acknowledge some discussions on charge exchange with Dr. C. B. Richardson.

APPENDIX A: DYNAMICS OF A BINARY ELASTIC COLLISION IN A HIGH-FREQUENCY FIELD

Let an ion of mass m_1 collide with another particle of mass m_2, where the amplitude of the high-frequency electric field is locally E, and let the scattering angle in the c.m. frame be θ_c. If the initial instantaneous velocities for the particles of mass m_1 and m_2 are, respectively, c_1 and zero, the final velocity of the ion is (in the laboratory frame)

$$\mathbf{c}_1'=\frac{m_2}{m_1+m_2}c_1\boldsymbol{\theta}+\frac{m_1}{m_1+m_2}\mathbf{c}_1, \tag{A1}$$

where $\boldsymbol{\theta}$ is a unit vector directed at an angle θ_c with respect to $\mathbf{c}_1$. The first term represents the final velocity in the c.m. frame, and the second term is the velocity of the c.m. Now the effect of the rf field is to make the velocity of the ion appear of the form

$$\mathbf{c}_1=\mathbf{u}+\mathbf{v}, \quad \mathbf{v}=(e/m_1\Omega)\mathbf{E}\sin\phi_{\mathrm{rf}}, \tag{A2}$$

where ϕ_{rf} is the phase of the rf field at the instant of collision. Substituting this form into the first equation yields, on squaring and regrouping of terms,

$$u'^2-u^2=-2\frac{m_1m_2}{(m_1+m_2)^2}(u^2+2\mathbf{u}\cdot\mathbf{v}+v^2)(1-\cos\theta) \\ -2(\mathbf{u}'-\mathbf{u})\cdot\mathbf{v}. \tag{A3}$$

Care must be taken at this point before carrying out an average over ϕ_{rf}, since $\mathbf{u}'$ is not uncorrelated with $\mathbf{v}$, and hence for the second term on the right we write

$$2(\mathbf{u}'-\mathbf{u})\cdot\mathbf{v}=2(\mathbf{c}_1'-\mathbf{c}_1)\cdot\mathbf{v}=2\frac{m_2}{m_1+m_2}(c_1\boldsymbol{\theta}-\mathbf{c}_1)\cdot\mathbf{v}. \tag{A4}$$

Now, carrying out the average over ϕ_{rf}, we obtain, using the fact that $(\mathbf{u}\cdot\mathbf{v})_{\mathrm{av}}=0$,

$$\langle u'^2-u^2\rangle_{\mathrm{av}}=-2\frac{m_1m_2}{(m_1+m_2)^2}\langle u^2+v^2\rangle_{\mathrm{av}}(1-\cos\theta_c) \\ +2\frac{m_2}{(m_1+m_2)}\langle v^2\rangle_{\mathrm{av}}(1-\cos\theta_c), \tag{A5}$$

from which the desired result immediately follows. The implied assumption here of a constant collision rate for encounters with fixed $\mathbf{u}$ and θ_c but varying $\mathbf{v}(t_1)$ is of course open to question.

APPENDIX B: FORMAL DERIVATION OF RATE EQUATIONS FOR $(He^3)^+$ hfs STATES

Let the density matrix representing the composite system consisting of $(He^3)^+$ ions with nuclear spin $I=\frac{1}{2}$ and Cs atoms be ρ. It may be assumed that there is no coherence between the electronic molecular states which are asymptotically $He^+ + Cs$ and $He^* + Cs^+$ and the molecular-spin states, and further it is expected that the presence of a nuclear spin for Cs will not alter significantly the results sought here; hence it will be assumed that $I=0$ for Cs. Thus, for the present purposes, the density matrix ρ may be written as

$$\rho=\rho_e\otimes\rho_s, \tag{B1}$$

where ρ_e is a 2×2 matrix representing the molecular electronic state and ρ_s is an 8×8 matrix representing the molecular-spin state (including the nuclear spin of the He^+, $I=\frac{1}{2}$).

The S matrix which transforms the initial state into the final state resulting from the collision according to

$$\rho=S\rho S^\dagger \tag{B2}$$

is related to the transition matrix T by the following:

$$S_{ij}=\delta_{ij}-2\pi i\delta(E_j-E_i)T_{ij}. \tag{B3}$$

For the present system the composite transition matrix will be taken to be given by

$$\frac{-\mu}{2\pi\hbar^2}T=\begin{pmatrix}f_{aa} & f_{ab}\\ f_{ba} & f_{bb}\end{pmatrix}\otimes P_3+\begin{pmatrix}g_{aa} & g_{ab}\\ g_{ba} & g_{bb}\end{pmatrix}\otimes P_1, \tag{B4}$$

where a, b label the two electronic molecular states, and P_1, P_3 are the projection operators for $S=0$, $S=1$, where S is the total electronic spin of the two-particle system. This may be written in terms of the Pauli matrices σ_1, σ_2; thus

$$\frac{-\mu}{2\pi\hbar^2}T=\begin{pmatrix}s_{aa} & s_{ab}\\ s_{ba} & s_{bb}\end{pmatrix}\otimes I+\begin{pmatrix}d_{aa} & d_{ab}\\ d_{ba} & d_{bb}\end{pmatrix}\otimes(\boldsymbol{\sigma}_1\cdot\boldsymbol{\sigma}_2), \tag{B5}$$

where

$$s_{ij}=\tfrac{3}{4}f_{ij}+\tfrac{1}{4}g_{ij},\quad d_{ij}=\tfrac{1}{4}(f_{ij}-g_{ij}).$$

The elements of the transition matrix also connect linear momentum states and should be labelled $f_{aa}(k',k)$, etc., omitted in the above for the sake of brevity. Now, under the actual physical conditions obtaining in the experiment, the Cs^+ ions are not confined by the trapping field, and their density can be taken to be at all times negligibly small; hence the initial density matrix may be assumed to have the form

$$(k''is''|\rho|k'js')=\delta(k'',k_0)\delta(k',k_0)\delta_{ia}\delta_{ja}\rho_{s''s'}. \tag{B6}$$

Moreover, only those elements of the transformed matrix ρ' which are of the form $(a|\rho'|a)$, corresponding to the Cs-He^+ electronic molecular state, are of interest, since the others are by the experimental circumstance mentioned above quickly reduced to zero. Thus only elements of S diagonal in the electronic molecular states will enter into the evaluation of these elements of ρ', which may now be carried out. The trace over k may be handled in a manner following Balling *et al.*,[28] leading to the following time-evolution equation for the submatrix consisting of these elements denoted by ρ_a:

$$\frac{d\rho_a}{dt}=vN\left\{\frac{2\pi i}{k}[M_{aa}(0)\rho_a-\rho_aM_{aa}^\dagger(0)]+\int M_{aa}\rho_aM_{aa}^\dagger d\Omega\right\}, \tag{B7}$$

where v is the relative velocity, N is the number density of atoms, and

$$M_{aa}=\tfrac{3}{4}f_{aa}+\tfrac{1}{4}g_{aa}+\tfrac{1}{4}(f_{aa}-g_{aa})(\boldsymbol{\sigma}_1\cdot\boldsymbol{\sigma}_2).$$

Written out in full, this expression may be regrouped to give (dropping the subscripts for brevity)

$$\frac{1}{vN}\frac{d\rho_a}{dt}=\left[\frac{2\pi i}{k}(s(0)-s^*(0))+\int|s|^2d\Omega\right]\rho_a-\left[\frac{2\pi i}{k}d^*(0)+\int sd^*d\Omega\right]\rho_a(\boldsymbol{\sigma}_1\cdot\boldsymbol{\sigma}_2)^\dagger$$
$$+\left[\frac{2\pi i}{k}d(0)+\int ds^*d\Omega\right](\boldsymbol{\sigma}_1\cdot\boldsymbol{\sigma}_2)\rho_a+\int|d|^2d\Omega(\boldsymbol{\sigma}_1\cdot\boldsymbol{\sigma}_2)\rho_a(\boldsymbol{\sigma}_1\cdot\boldsymbol{\sigma}_2)^\dagger. \tag{B8}$$

The expression on the right can now be put in a more useful form by applying the optical theorem[29] in the form appropriate to the present problem, namely,

$$\int(|f_{aa}|^2+|f_{ab}|^2)d\Omega=-\frac{2\pi i}{k}[f_{aa}(0)-f_{aa}^*(0)] \tag{B9a}$$

and

$$\int(|g_{aa}|^2+|g_{ab}|^2)d\Omega=-\frac{2\pi i}{k}[g_{aa}(0)-g_{aa}^*(0)]. \tag{B9b}$$

[28] L. C. Balling, R. J. Hanson, and F. M. Pipkin, Phys. Rev. **133**, A607 (1964).
[29] A. Messiah, *Quantum Mechanics* (North-Holland Publishing Co., Inc., Amsterdam, 1963), Vol. II, p. 866.

TABLE II. The matrix $\boldsymbol{\sigma}_1\cdot\boldsymbol{\sigma}_2$ in the $|IJFM_F\rangle|sm_s\rangle$ representation for the $(He^3)^+$-Cs system.

	$1,1;+\frac{1}{2}$	$1,0;+\frac{1}{2}$	$1,-1;+\frac{1}{2}$	$0,0;+\frac{1}{2}$	$1,1;-\frac{1}{2}$	$1,0;-\frac{1}{2}$	$1,-1;-\frac{1}{2}$	$0,0;-\frac{1}{2}$
$1,1;+\frac{1}{2}$	1	0	0	0	0	0	0	0
$1,0;+\frac{1}{2}$	0	0	0	1	$2^{1/2}$	0	0	0
$1,-1;+\frac{1}{2}$	0	0	−1	0	0	$2^{1/2}$	0	$2^{1/2}$
$0,0;+\frac{1}{2}$	0	1	0	0	$-2^{1/2}$	0	0	0
$1,1;-\frac{1}{2}$	0	$2^{1/2}$	0	$-2^{1/2}$	−1	0	0	0
$1,0;-\frac{1}{2}$	0	0	$2^{1/2}$	0	0	0	0	−1
$1,-1;-\frac{1}{2}$	0	0	0	0	0	0	1	0
$0,0;-\frac{1}{2}$	0	0	$2^{1/2}$	0	0	−1	0	0

Thus, as a typical reduction, consider the coefficient of $\rho_a(\boldsymbol{\sigma}_1\cdot\boldsymbol{\sigma}_2)^\dagger$. This is

$$\frac{-2\pi i}{k}\times\tfrac{1}{4}(f_{aa}^*-g_{aa}^*)+\int(\tfrac{3}{4}f_{aa}+\tfrac{1}{4}g_{aa})\tfrac{1}{4}(f_{aa}^*-g_{aa}^*)d\Omega=\frac{-2\pi i}{k}\tfrac{1}{4}(f_{aa}^*-g_{aa}^*)+\int[\tfrac{1}{4}(f_{aa}-g_{aa})+\tfrac{1}{2}(f_{aa}+g_{aa})]$$

$$\times\tfrac{1}{4}(f_{aa}^*-g_{aa}^*)d\Omega=\frac{-2\pi i}{k}\tfrac{1}{4}(f_{aa}^*-g_{aa}^*)+\int\tfrac{1}{16}|f_{aa}-g_{aa}|^2+\tfrac{1}{8}[|f_{aa}|^2-|g_{aa}|^2-(f_{aa}g_{aa}^*-f_{aa}^*g_{aa})]d\Omega.$$

Using now the optical theorem, this can be put

$$=\int\tfrac{1}{16}|f_{aa}-g_{aa}|^2+\tfrac{1}{8}|g_{ab}|^2-\tfrac{1}{8}|f_{ab}|^2d\Omega-\int\tfrac{1}{8}(f_{aa}g_{aa}^*-f_{aa}^*g_{aa})d\Omega+\frac{2\pi i}{k}\tfrac{1}{8}[(g_{aa}+g_{aa}^*)-(f_{aa}+f_{aa}^*)]. \quad \text{(B10)}$$

Defining Q_e, Q_1, and Q_3 in a manner to conform with the usage in text,

$$Q_e=\tfrac{1}{4}\int|f_{aa}-g_{aa}|^2d\Omega,$$

$$Q_3=\int|f_{ab}|^2d\Omega, \quad \text{(B11)}$$

$$Q_1=\int|g_{ab}|^2d\Omega,$$

we find, after evaluating the other coefficients in a similar manner and collecting terms,

$$\frac{1}{vN}\frac{d\rho_a}{dt}=(-\tfrac{3}{4}Q_e-\tfrac{3}{4}Q_3-\tfrac{1}{4}Q_1)\rho_a$$
$$+\tfrac{1}{4}[Q_e+\tfrac{1}{2}(Q_1-Q_3)-iH]\rho_a(\boldsymbol{\sigma}_1\cdot\boldsymbol{\sigma}_2)^\dagger$$
$$+\tfrac{1}{4}[Q_e+\tfrac{1}{2}(Q_1-Q_3)+iH](\boldsymbol{\sigma}_1\cdot\boldsymbol{\sigma}_2)\rho_a$$
$$+\tfrac{1}{4}Q_e(\boldsymbol{\sigma}_1\cdot\boldsymbol{\sigma}_2)\rho_a(\boldsymbol{\sigma}_1\cdot\boldsymbol{\sigma}_2)^\dagger, \quad \text{(B12)}$$

where

$$H=\frac{1}{2i}\int(f_{aa}g_{aa}^*-f_{aa}^*g_{aa})d\Omega$$
$$-\frac{\pi}{k}[(g_{aa}+g_{aa}^*)-(f_{aa}+f_{aa}^*)].$$

Since we are interested in the evolution of the $(He^3)^+$-ion hfs substates, we require the matrix of the operator $\boldsymbol{\sigma}_1\cdot\boldsymbol{\sigma}_2$ in the $|IJFM_F\rangle|sm_s\rangle$ representation, which is given in Table II. Now, the simplest matrix which can be assumed for ρ_a, one which is consistent with the time-evolution equations, having elements which remain zero if initially zero, will have off-diagonal elements connecting only the (1,0), (0,0) states of the He^+ ion. Inserting these matrices in the rate equation for ρ_a, carrying out the indicated products, and taking the trace over the m_s of the Cs atom, one finds the following rate equations for the $(He^3)^+$ substates:

$$\frac{1}{vN}\dot\rho_{11}=-Q_T\rho_{11}+PQ_D\rho_{11}$$
$$+\tfrac{1}{4}Q_e(1+P)(\rho_{22}+\rho_{44}-\rho_{24}-\rho_{42}),$$
$$\frac{1}{vN}\dot\rho_{22}=-(Q_T+\tfrac{1}{4}Q_e)\rho_{22}+\tfrac{1}{4}PQ_e(\rho_{33}-\rho_{11})$$
$$+\tfrac{1}{4}Q_e(\rho_{11}+\rho_{33}+\rho_{44})+\tfrac{1}{2}PQ_D(\rho_{24}+\rho_{42})$$
$$-\tfrac{1}{4}iHP(\rho_{24}-\rho_{42}), \quad \text{(B13)}$$
$$\frac{1}{vN}\dot\rho_{33}=-Q_T\rho_{33}-PQ_D\rho_{33}$$
$$+\tfrac{1}{4}Q_e(1-P)(\rho_{22}+\rho_{44}+\rho_{24}+\rho_{42}),$$
$$\frac{1}{vN}\dot\rho_{44}=-(Q_T+\tfrac{1}{4}Q_e)\rho_{44}+\tfrac{1}{4}PQ_e(\rho_{33}-\rho_{11})$$
$$+\tfrac{1}{4}Q_e(\rho_{11}+\rho_{33}+\rho_{22})+\tfrac{1}{2}PQ_D(\rho_{24}+\rho_{42})$$
$$+\tfrac{1}{4}iHP(\rho_{24}-\rho_{42}),$$

where the states have been numbered in the order α, β, ν, δ, and Q_T and Q_D are defined as follows:

$$Q_T=\tfrac{1}{2}Q_e+\tfrac{3}{4}Q_3+\tfrac{1}{4}Q_1, \quad Q_D=\tfrac{1}{2}Q_e+\tfrac{1}{4}(Q_1-Q_3).$$

To verify that these equations reduce to the equations derived in the text, we must put $Q_1=Q_3=0$, that is, $Q_T=Q_D=\frac{1}{2}Q_e$. Then it is evident that on ignoring the off-diagonal elements, which the derivation in the text did not claim to yield, the results are identical. The off-diagonal elements ρ_{24}, ρ_{42} have the following rate equations:

$$\frac{1}{vN}\dot{\rho}_{24}=-Q_T\rho_{24}+\tfrac{1}{4}Q_e(\rho_{33}-\rho_{11})+\tfrac{1}{4}Q_eP(\rho_{33}+\rho_{11})+\tfrac{1}{2}Q_DP(\rho_{22}+\rho_{44})-\tfrac{1}{4}iHP(\rho_{22}-\rho_{44})+\tfrac{1}{4}Q_e\rho_{42}, \quad \text{(B14)}$$

$$\dot{\rho}_{42}=\dot{\rho}_{24}^{*}.$$

It should be noted that under the existing experimental conditions, where a given Cs atom in the beam spends a time in the interaction region negligibly short compared with the spin-exchange time, the phase coherence between the spin states of the Cs atom and the He^+ ion cannot develop. Therefore the off-diagonal terms corresponding to this coherence have been presumed zero at all times.

APPENDIX C: RESPONSE OF HARMONICALLY BOUND IONS TO DETECTION FIELD

In the approximation of a uniform detection field, which may be thought of as produced between the parallel plates of a condenser, the motion of the center of charge with an instantaneous velocity $\dot{z}_c$ will cause the flow of a current in the external resistance R_r given by

$$i=ne\dot{z}_c/2z_0, \quad \text{(C1)}$$

where $2z_0$ is here taken to approximate the condenser plate separation. Thus, if the externally applied field is $Ee^{i\omega t}$, the total field acting on the ions will be

$$E'(t)=Ee^{i\omega t}-neQ/(4z_0^2\omega C)\dot{z}_c. \quad \text{(C2)}$$

Now the equation of motion for the jth ion is given by

$$\ddot{z}_j+\omega_0^2z_j=\frac{eEe^{i\omega t}}{m}-ne^2Q/(4mz_0^2\omega C)\dot{z}_c=\gamma e^{i\omega t}-k\dot{z}_c. \quad \text{(C3)}$$

Since E is assumed to be independent of z_j, we may sum the equations for all j and obtain simply

$$\ddot{z}_c+\omega_0^2z_c=\gamma e^{i\omega t}-k\dot{z}_c. \quad \text{(C4)}$$

To introduce the vector amplitude Z_c as defined in the text, we require the derivatives of z_c; thus

$$\dot{z}_c=(i\omega Z_c+\dot{Z}_c)e^{i\omega t},$$
$$\ddot{z}_c=(-\omega^2Z_c+2i\omega\dot{Z}_c+\ddot{Z}_c)e^{i\omega t}.$$

Inserting these expressions in Eq. (C4) and writing $\omega_0=\omega-\Delta$, we find, assuming $\Delta/\omega\ll1$ and Z_c to be a slowly varying function of the time,

$$[1-(ik/2\omega)]\dot{Z}_c+(\tfrac{1}{2}k+i\Delta)Z_c=-i\gamma/2\omega, \quad \text{(C5)}$$

and multiplying through by $[1+(ik/2\omega)]$, we obtain the result given in the text.